SUPPLEMENTAL EXPERIMENTAL PROCEDURES

Cell line transfections and naïve cell transductions. Jurkat cells were transiently transfected by electroporation as described previously (Borroto et al., 1999). For lentiviral transductions, transducing supernatants were produced from transfected packaging HEK293T cells as described (Martinez-Martin et al., 2009). The pHR-CD3ζGFP construct expressing CD3ζ fused at the C-terminus to GFP was co-transfected in HEK293T cells together with vectors expressing HIV gag/pol genes and the VSV G protein. To transduce naïve T cells, lymph node cells from *RRAS2*$^{-/-}$ and *RhoG*$^{-/-}$ mice were resuspended at 5x10^5 cells/ml in filtered transducing supernatant, 1 μg/ml anti-CD3 145-2C11 was added and the cells were centrifuged for 90 min at 1500g at 32^{o}C. The cells were maintained in the same medium for 6 h at 37ºC, and they were then washed and diluted in RPMI supplemented with 5 pg/ml IL-2. The transduced T cells were then used 3-4 days later.

Clathrin heavy chain knockdown. For siRNA transfections, 20 x 10^6 Jurkat cells were washed twice with cold RPMI free of FCS, and resuspended in 400 μl of Opti-MEM-1 medium (Gibco) containing 0.5 μM each of siRNAs GGCUCAUACCAUGACUGAU and GGGUGCCAGAUUAUCAAUU (Ambion). Cells were electroporated at 250 mV/ 1000 μF and used 48 h after transfection.

T cell stimulation and flow cytometry. The expression of CD69 at the membrane of CD4$^+$ cells was analyzed 24h after stimulation with 5x10^4 DCEK cells preloaded with different concentrations of MCC peptide, or with beads of different sizes coupled to the 145-2C11 anti-CD3 antibody. Cells were incubated with an antibody against CD69 and they were analyzed in a FACSCalibur (Becton Dickinson) flow cytometer. The culture supernatant of stimulated T cells was collected after 24 hours to measure IL-2 release,

which was analyzed using an ELISA kit (Bender Medsystems). T cell proliferation in response to either antigen or beads was measured by CFSE dye dilution after 72h at 37^{o}C. The proliferation index was calculated according to the number of cell divisions and the percentage of cells in each CFSE peak of the $CD4^{+}$ population.

TCR downmodulation. DCEK cells preloaded overnight with different concentrations of MCC were plated on flat bottom 96 well plates ($5x10^{4}$ cells per well) and used as presenting cells. DCEK cells were washed with PBS and lymph node naïve T naive cells ($2x10^{5}$ cells per well) were added. After the appropriated incubation time the cells were stained for CD4 and Vβ3 TCR, and they were analyzed by FACS.

Immunoblot analysis of T cell activation. A total of $3x10^{7}$ naïve CD4 T cells of each genotype were activated at different times with DCEK cells preloaded with 10 μM MCC. After different incubation times, the cells were lysed in 1 ml of Brij96 lysis buffer containing protease and phosphatase inhibitors (1% Brij96, 140 mM NaCl, 10 mM Tris–HCl [pH 7.8], 10 mM iodoacetamide, 1 mM PMSF, 1 μg/ml leupeptin, 1 μg/ml aprotinin, 1 mM sodium orthovanadate, 20 mM sodium fluoride and 5 mM of $MgCl_2$). Immunoblotting was performed as described previously (Martinez-Martin et al., 2009). Pull-down with GST-ELMO was performed as described (Prieto-Sanchez et al., 2006).

Electron microscopy. Jurkat cells (20×10^{6}) were allowed to ingest anti-CD3 coated latex beads (1μm) for different times (5, 15, 30 and 60 minutes) using a cell:bead ratio of 1:50 (see Experimental Procedures). Cell pellets were fixed *in situ* with 4% paraformaldehyde in 0.1M phosphate buffer [pH 7.4] for 1.5 h at room temperature and then overnight in 8% paraformaldehyde at 4ºC. Fixed cells were washed and embedded in 10% gelatin in PBS. Approximately 0.5 -1 mm^{3} cubes of gelatin embedded cells were

cryoprotected with 15 % glycerol for 15 min and for an additional 15 min. in 30% glycerol, before they were plunge freezed in liquid propane and immediately transferred to an Automatic Freeze-Substitution System (AFS, Leica). Freeze substitution was carried out at -85ºC in methanol containing 0.5% uranyl acetate for 54 hr. After raising the temperature to -45ºC at a rate of 5º C/h, and washing several times with pure methanol, the samples were infiltrated with Lowicryl HM20 and polymerized by UV light irradiation at -45ºC for two days. Ultrathin Lowicryl sections were cut in a Reichert-Jung Ultracut E ultramicrotome and the samples were examined at 80Kv with a JEM 1010 electron microscope.

For electron microscopy of T cells stimulated on patterned arrays we followed the procedure described in (Doh and Irvine, 2006). Basically, lymph node C57BL/6 mouse T cells were plated on patterned arrays containing a central anti-CD3 spot surrounded by ICAM-1. Cells were plated and sat on the surfaces aligned with the spots. Cells were unroofed using a probe sonicator and then fixed for freeze etch EM. More vigorous sonication was used to remove the actin ring and allow visualization of clathrin cages.

Intensity Correlation Analysis. In brief, Pearson´s Correlation Coefficient (PC) is a standard statistical analysis designed to measure the strength of a linear relationship between two variables, in this case fluorescent intensities from two images. To calculate PC for a pair of fluorescence images, all of the pixels having the same image coordinates are paired. The mean pixel intensity of an image is subtracted from the intensity of each pixel within the image, and the value generated for each pixel is multiplied by the equivalent value from the pixel's partner in the counterpart image to generate the product of the difference from the mean. The product of the difference from the mean is summed for the entire dataset and divided by the maximum possible

sum of the product of the difference from the mean (Adler et al., 2008). PC generates a range of values from 1, a perfect positive correlation, to −1, a perfect but inverse correlation, with 0 representing a random distribution. Taking into account that PC rarely discriminates differences between partial colocalization or exclusion, especially if images contain noise (Bolte and Cordelieres, 2006), we took advantage of a new correlation method "ICA" in order to circumvent those drawbacks. The ICA method is based on the principle that if two proteins are parts of the same complex then their staining intensities should vary in synchrony, whereas if they are on different complexes or structures they will exhibit asynchronous staining. ICA analysis involves generating scatter-plots of stain A or stain B against the product of the difference of each pixel A and B intensities from their respective means. The resulting plots emphasize the high intensity stained pixels and allow us to identify protein pairs that vary in synchrony, randomly, or independently within the cell. In addition, to complement ICA results, Intensity Correlation Quotient (ICQ) was used to provide an overall index of whether the staining intensities are associated in a random, a dependent or a segregated manner (for more details see (Li et al., 2004)). As a final point, it must be noted that as PC values depend upon a simple linear relationship, they will be depressed if measured over a field of cells with heterogeneous expression or uptake of the target molecules, thus under-representing the degree of correlation; to circumvent this, regions of interest (ROIs, 5x6 μm) within the cell were drawn when necessary. Moreover, it has been widely demonstrated that carefully outlining the region in which two probes may potentially distribute is critical to accurate measurement of PC (Dunn et al.).

Coupling antibodies to latex beads. Fluorescent latex beads of 1, 3 and 6 μm diameter purchased from the commercial sources indicated in the following table were derivatized using a C-terminal carboxy coupling kit (Microparticles, Polysciences). The

derivatized beads were incubated with purified monoclonal antibodies at a concentration of 300 μg/ml. After incubation overnight, the beads were processed according to the supplier's instructions and the concentration of protein in the supernatant was measured to calculate the efficiency of immobilization onto the beads.

Table of Beads used:

Name	Origin	Size	Ext/ems
Polybead Carboxylate Microspheres	Polyscience, Inc.	1 μm	--
FluoroSpheres® Carboxylate-modified microspheres, crimson fluorescent	Molecular Probes	1 μm	625/645
Fluoresbrite® Carboxylate Microspheres.	Polyscience, Inc.	3 μm	529/546
Fluoresbrite® Carboxylate Microspheres.	Polyscience, Inc.	6 μm	529/546

Antibodies and other materials:

Antibody	**Clone or code nº**	**Description**	**Use**	**Origin**
Anti-CD3ζ	448	Rb polyclonal	WB/IF	San José et al. 1998
Anti-Mouse CD3	145-2C11	Hamster mAb	Beads	J. Bluestone, UCSF
H57-FITC, biotinylated	H57-597	Hamster mAb	FC/IF	Immunotools Bioscience.
CD4-PE -PerCP -Biotinylated	RM4-5	Rat mAb	FC	BD Pharmingen
CD8α-FITC, -PE, -PerCP, -Biotinylated	53-6.7	Rat mAb	FC	BD Pharmingen
Clathrin Heavy Chain	23	Mouse mAb	IF	BD Pharmingen
OKT 3		Mouse mAb	Beads	Ortho Diagnostic Systems (Raritan, NJ).
FG 1/6		Mouse mAb	Beads	(Salmeron et al., 1995)
OKT 8		Mouse mAb	Beads	Ortho Diagnostic Systems (Raritan, NJ).
Vβ 3 TCR PE Biotinylated	KJ25	Mouse mAb	FC	BD Pharmingen
CD69 FITC Biotinylated	H1.2F3	Hamster mAb	FC	BD Pharmingen
Phospo-Zap70 (Tyr319)/Syk (Tyr352)	65E4	Rabbit mAb	WB	Cell Signalling
RhoG	1F3 B3 E5	Mouse mAb	WB	Santa Cruz

				Biotechnology, INC.
RhoG	C-20	Rabbit polyclonal	IF	Santa Cruz Biotechnology, INC.
Phospo-p44/42 MAP Kinase (thr202/Tyr204) antibody		Rabbit mAB	WB	Cell Signalling
p44/42 MAP Kinase antibody		Rabbit mAB	WB	Cell Signalling
4G10	4G10	Mouse mAb	WB	
I-E^K Biotinylated	17-3-3	Mouse mAb	FC	BD Pharmingen
B220 Biotinylated	RA3-6B2	Rat mAb	FC	BD Pharmingen
CD11b Biotinylated	M1/70	Rat mAb	FC	BD Pharmingen
CD11c Biotinylated	HL3	Hamster mAb	FC	BD Pharmingen
Anti-hamster FITC	127-095-160	Goat anti-Armenian hamster IgG	FC/IF	Jackson Immunoresearch
Alexa 488	A-21206	Donkey anti-rabbit IgGs	IF	Invitrogen
Alexa 488	A-21202	Donkey anti-mouse IgGs	IF/FC	Invitrogen
Alexa 555	A-31572	Donkey anti-rabbit IgGs	IF	Invitrogen
Alexa 555	A-31570	Donkey anti-mouse IgGs	IF	Invitrogen
Alexa 555	S-32355	Streptavidin	IF	Invitrogen
Alexa 488	S-11223	Streptvidin	IF	Invitrogen
Alexa 594	A-21207	Donkey anti-rabbit IgGs	IF	Invitrogen
Alexa 594	A-21203	Donkey anti-mouse IgGs	IF	Invitrogen
Alexa 647	A-31573	Donkey anti-rabbit IgGs	IF	Invitrogen
Other Materials:	**Code nº**	**Description**	**Use**	**Origin**
To-Pro-3	T-3605	Monomeric Cyanine Nucleic Acid Stain	IF	Invitrogen
Alexa Fluor® 488 phalloidin	A-12379	Probe for F-Actin	IF	Invitrogen
Phalloidin–Tetramethylrhodamine B isothiocyanate	P-1951	Probe for F-Actin	IF	Sigma
Mouse IL-2 Platinum ELISA	BMS601			Bender Medsystems
CFSE			FC	Molecular Probes
PKH26 Red Fluorescent Cell Linker Kit.	PKH26GL	Fluorescent Cell Linker Dyes	FC/IF	Sigma
Transferrin from human serum, Alexa Fluor® 633 conjugate	T-23362	Transferrin Conjugate	IF	Molecular Probes
Cytochalasin D	250255	Inhibitor of actin	FC	Calbiochem

		filament function.		
Wortmannin	681675	Irreversible inhibitor of phosphatidylinositol 3-kinase	FC	Calbiochem
LY 294002	440202	Reversible and specific phosphatidyl-inositol 3-kinase inhibitor	FC	Calbiochem
MCC Peptide		ANERADLIAYL KQATK		
OVA Peptide		SIINFEKL		
Glass Bottom Culture Dishes		35mm Petri dish 10mm microwell	IF	MatFek Coorporation

Table of plasmids:

Name	Plasmid	Origin	Description
TC21 WT-Dsred, -GFP, -CFP	pDsred2-C1 pEGFP-C1 pECFP-C1	PCR cloning of the wild type human cDNA sequence into the plasmid.	WT form of TC21.
TC21 S28N-Dsred, -GFP, -CFP	pDred2-C1 pEGFP-C1 pECFP-C1	Introducing a S28N mutation using the Site Directed mutagenesis Kit(Statagene).	Dominant inactive form of TC21.
TC21 G23V.Dsred, -GFP, -CFP	pDsred2-C1 pEGFP-C1 pECFP-C1	Introducing a G23V mutation using the Site Directed mutagenesis Kit(Statagene).	Constitutively active form of TC21.
RhoG WT-GFP, -CFP	pEGFP-C1 pECFP-C1	(Prieto-Sanchez et al., 2006)	WT form of RhoG.
RhoG T17N-GFP, -CFP	pEGFP-C1 pECFP-C1	(Prieto-Sanchez et al., 2006)	Dominant inactive form of RhoG.
RhoG Q61L-GFP. -CFP	pEGFP-C1 pECFP-C1	(Prieto-Sanchez et al., 2006)	Constitutively active form of RhoG.
CD3-ζ-GFP, -CFP , -Dsred, -Cherry	pDsred2-N1 pEGFP-N1 pECFP-N1 pmCherry-N1	cDNA insertion into XhoI and EcoRI sites of indicated vectors.	
pHR-CD3ζGFP	pHRSIN-CSGW	cDNA insertion into BamHI and NotI sites of plasmid pHRSIN-CSGW-dlNotI	CD3ζ GFP fusion protein
Rab4, 5, 7 and 11 -GFP	pEGFPC1-N1	Marino Zerial, Max Planck Institute of Molecular Cell Biology and Genetics, Germany	WT forms of Rabs 4, 5, 7 and 11

References

Adler, J., Pagakis, S.N., and Parmryd, I. (2008). Replicate-based noise corrected correlation for accurate measurements of colocalization. J Microsc. *230*, 121-133.

Bolte, S., and Cordelieres, F.P. (2006). A guided tour into subcellular colocalization analysis in light microscopy. J Microsc. *224*, 213-232.

Borroto, A., Lama, J., Niedergang, F., Dautry-Varsat, A., Alarcon, B., and Alcover, A. (1999). The CD3 epsilon subunit of the TCR contains endocytosis signals. J Immunol *163*, 25-31.

Doh, J., and Irvine, D.J. (2006). Immunological synapse arrays: patterned protein surfaces that modulate immunological synapse structure formation in T cells. Proc Natl Acad Sci U S A. *103*, 5700-5705. Epub 2006 Apr 5703.

Dunn, K.W., Kamocka, M.M., and McDonald, J.H. A practical guide to evaluating colocalization in biological microscopy. Am *300*, C723-742. Epub 2011 Jan 2015.

Li, Q., Lau, A., Morris, T.J., Guo, L., Fordyce, C.B., and Stanley, E.F. (2004). A syntaxin 1, Galpha(o), and N-type calcium channel complex at a presynaptic nerve terminal: analysis by quantitative immunocolocalization. J Neurosci. *24*, 4070-4081.

Martinez-Martin, N., Risueno, R.M., Morreale, A., Zaldivar, I., Fernandez-Arenas, E., Herranz, F., Ortiz, A.R., and Alarcon, B. (2009). Cooperativity between T cell receptor complexes revealed by conformational mutants of CD3epsilon. Sci Signal. *2*, ra43.

Prieto-Sanchez, R.M., Berenjeno, I.M., and Bustelo, X.R. (2006). Involvement of the Rho/Rac family member RhoG in caveolar endocytosis. Oncogene. *25*, 2961-2973.
Salmeron, A., Borroto, A., Fresno, M., Crumpton, M.J., Ley, S.C., and Alarcon, B. (1995). Transferrin receptor induces tyrosine phosphorylation in T cells and is physically associated with the TCR zeta-chain. J Immunol *154*, 1675-1683.

Supplemental Fig S1

A

Time (min):

CD3ζ TC21wt

20

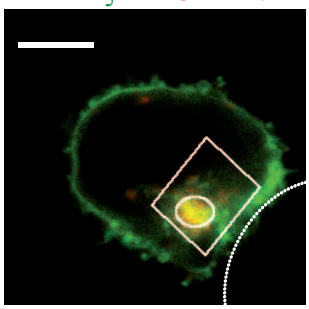

Area 1

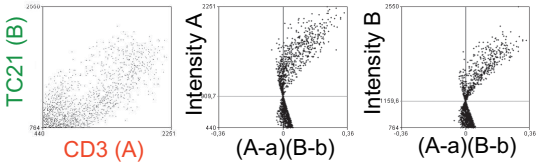

PC= +0.722 ICQ= +0.291

Vesicle 2

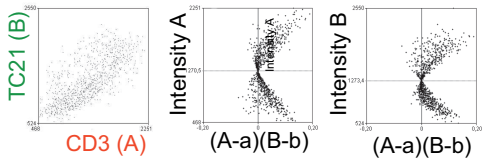

PC= +0.720 ICQ= +0.237

B

Time (min):

TC21 S28N CD3ζ

23

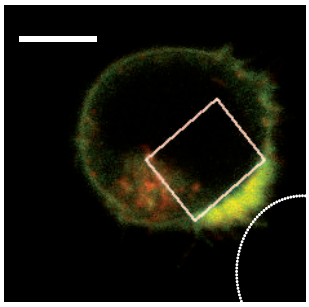

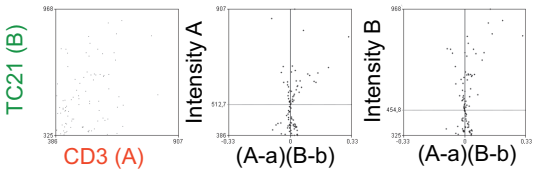

PC= +0.029 ICQ= +0.012

C

Time (min):

TC21 G23V CD3ζ

20.5

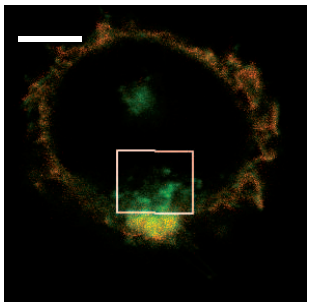

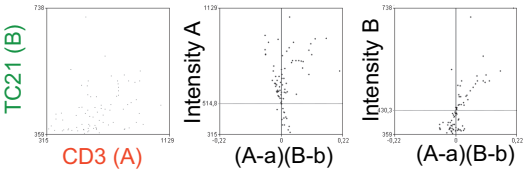

PC= +0.030 ICQ= +0.010

D

Time (min):

RhoG wt CD3ζ

25.5

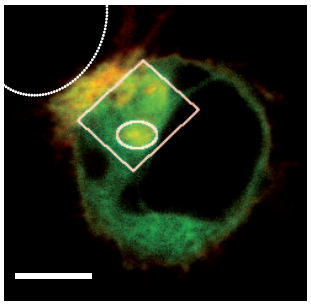

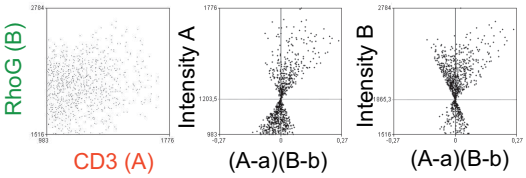

PC= +0.144 ICQ= +0.025

Vesicle 2

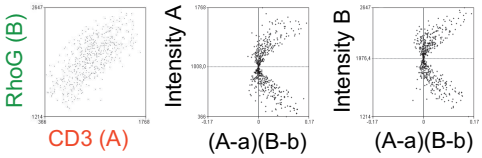

PC= +0.676 ICQ= +0.236

Supplementary Fig. S1

Supplemental Fig S2

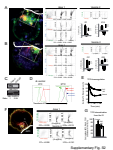

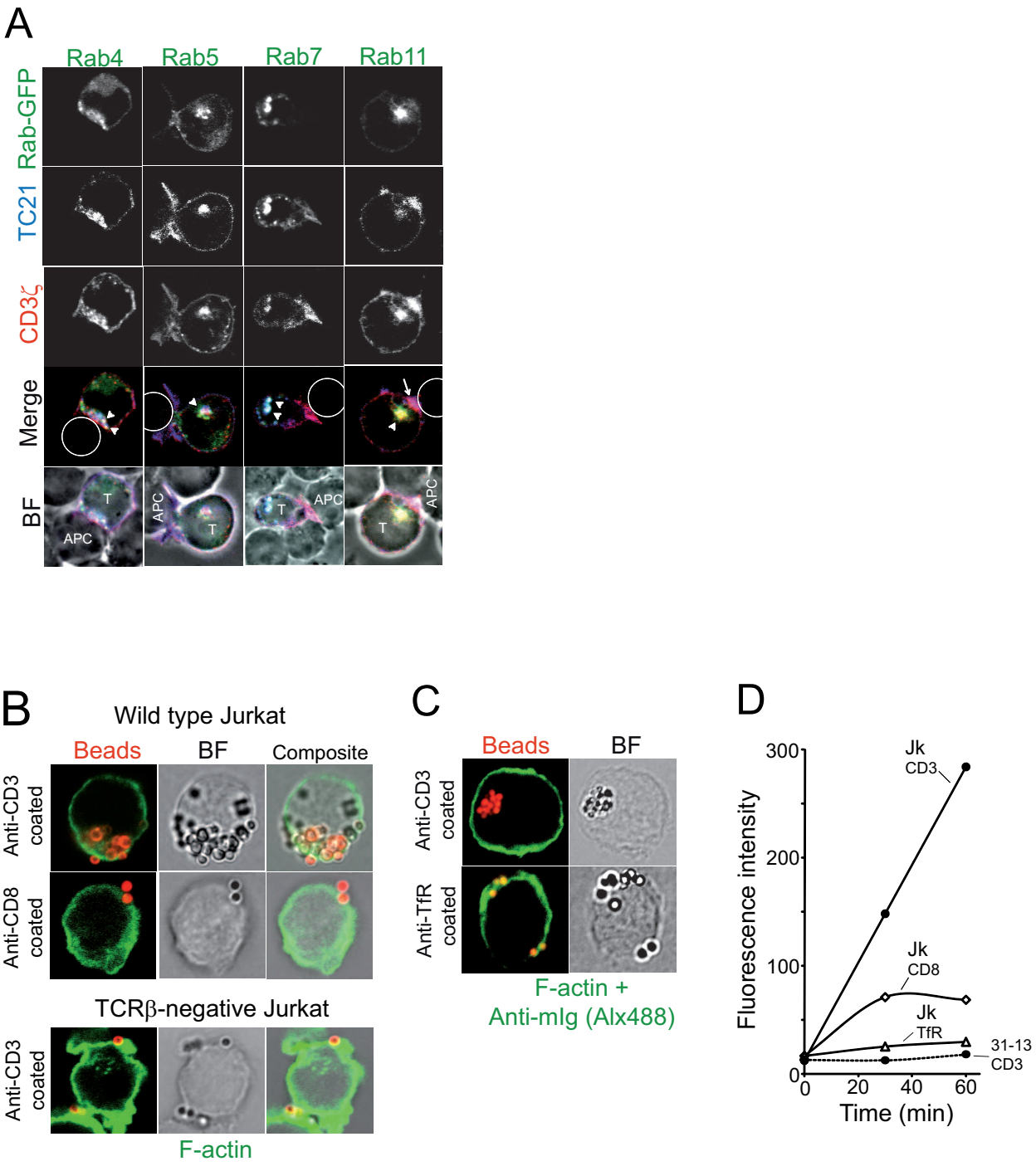

Supplementary Fig. S3

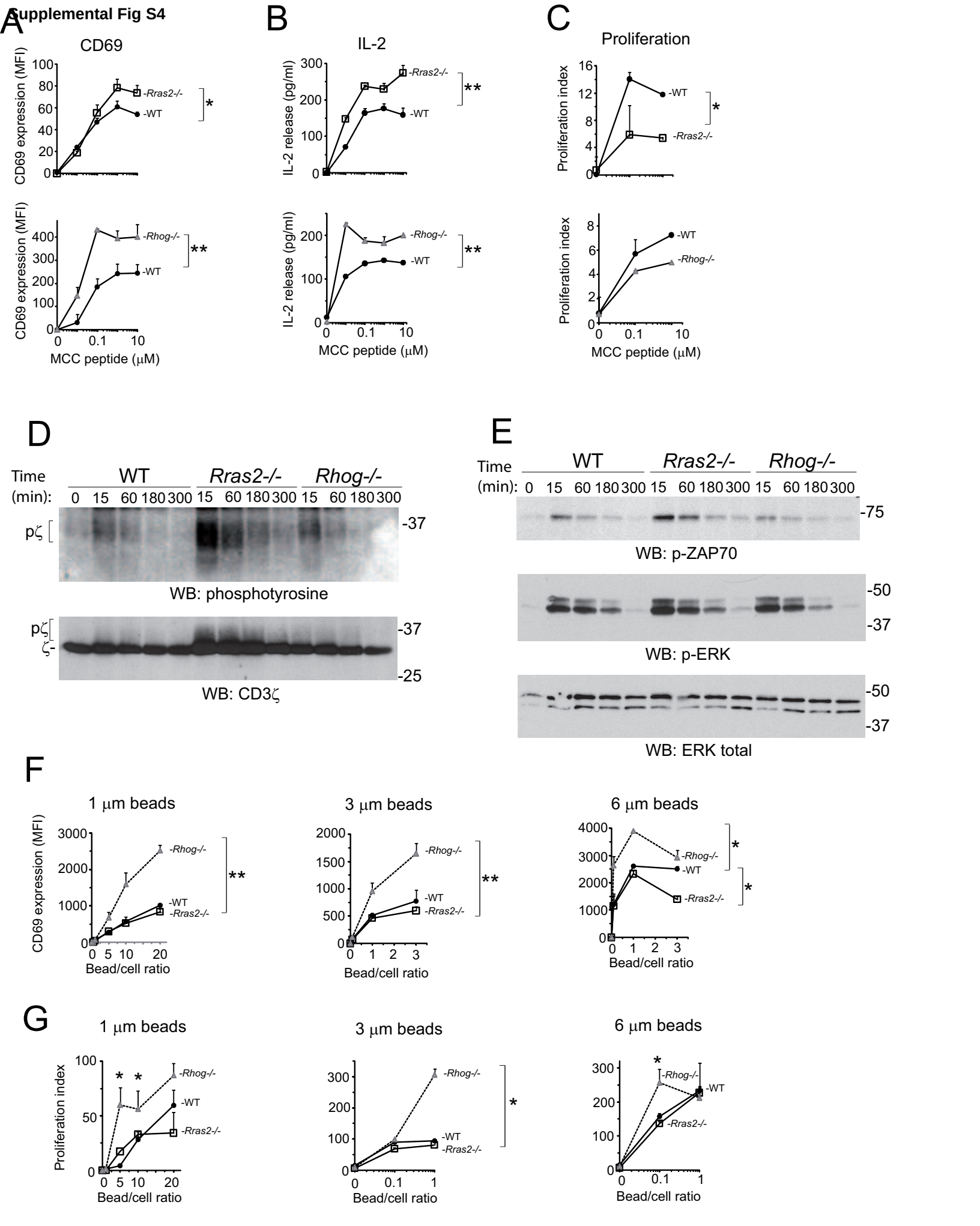

Supplementary Fig. S4

A

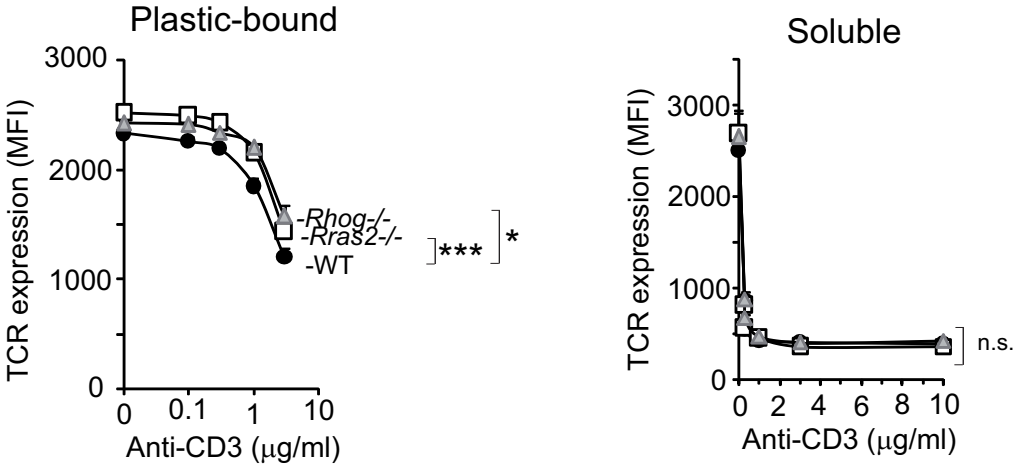

B

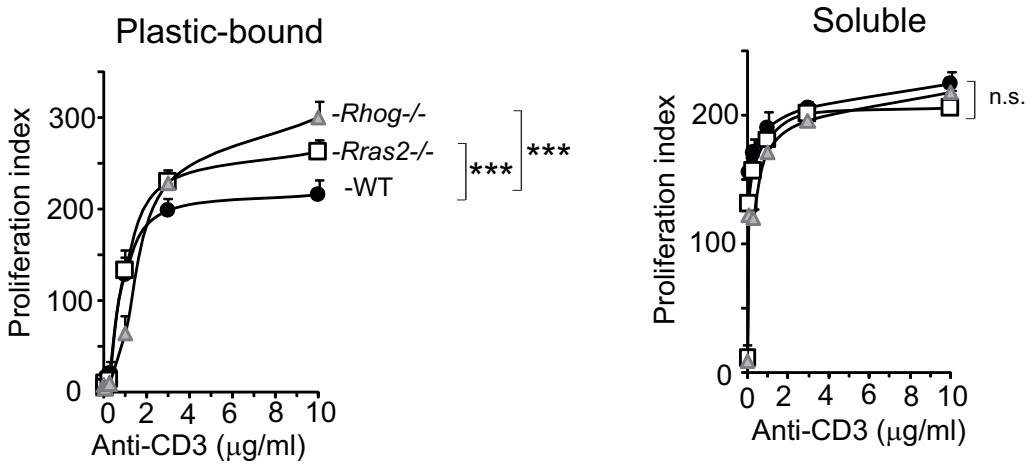

Supplementary Fig. S5

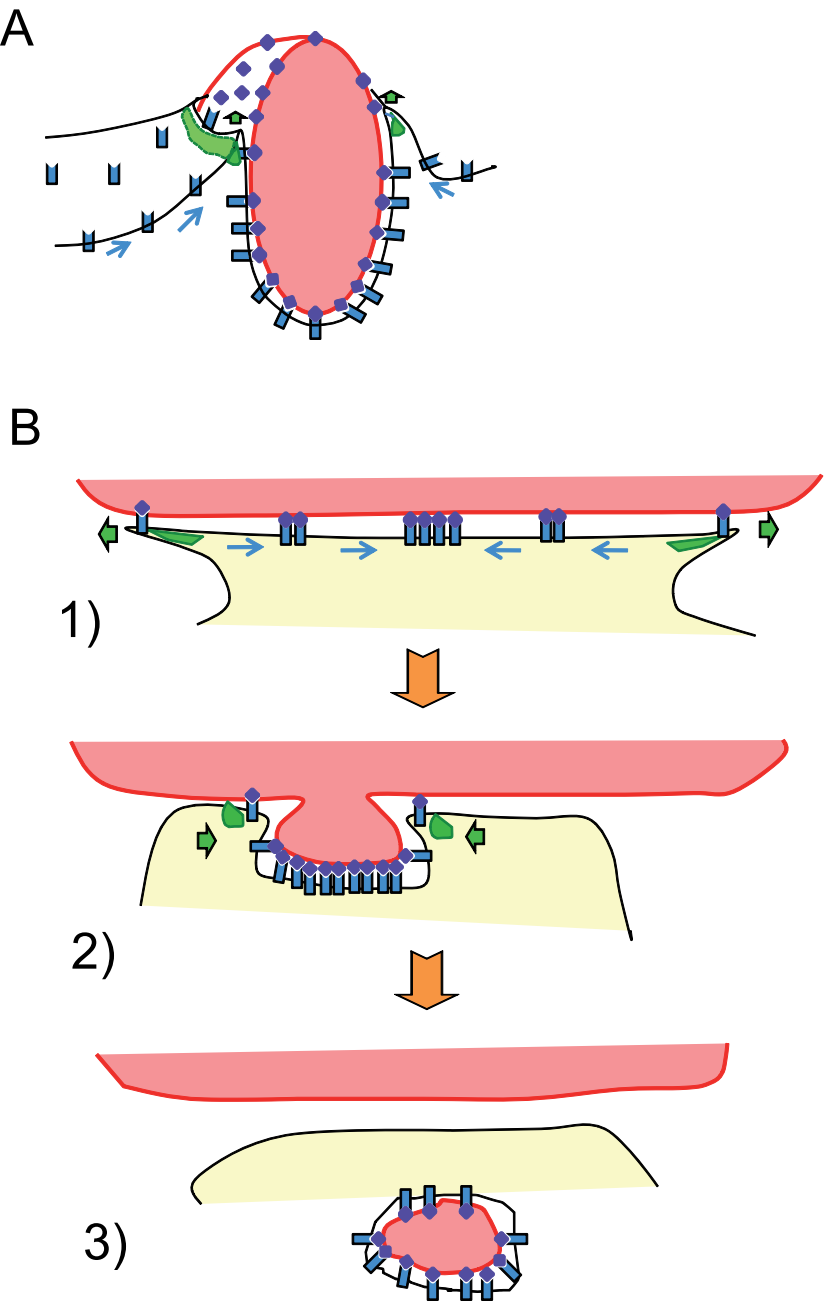

Supplementary Fig. S6

LEGENDS TO SUPPLEMENTAL FIGURES AND MOVIES

Suppl. Figure S1. Co-localization analysis. **(A)** TC21 and CD3ζ co-localize at the IS and are internalized in common vesicles. Jurkat cells were co-transfected with TC21-GFP and CD3ζ-Cherry and stimulated with SEE-loaded Raji cells. Conjugated formation was recorded by confocal microscopy (see material and methods) taking different time points. Intensity correlation analysis (ICA) for TC21 signal compared with CD3ζ signal was performed. Pearson's Coefficient (PC) and intensity correlation coefficient (ICQ) values were obtained from region of interest 1 (area 1) and individual vesicles (vesicle 2) 20 min after the Jurkat:Raji contact was initiated. Scale bar-5 μm. After analyzing the co-localization coefficients in double positive vesicles (vesicle 2) originated at the IS in different cells (n=10), we obtained a PC of +0.720±0.027 (Mean±SEM), illustrated by the highly correlated scatter plot or fluorogram shown for area 1 at time point 20. In addition, we obtained an average ICQ value of +0.237±0.017, illustrated by (A-a)(B-b) plots strongly skewed toward positive values as shown for area 1. Overall, the ICA shows that TC21 and CD3ζ co-localize in IS-derived internal vesicles. **(B & C)** TC21 mutants that are constitutively in the GDP (S28N mutant) and GTP (G23V mutant) forms co-localized with CD3ζ at the IS but blocked its internalization. Transfection and co-localization analysis were performed as in panel A. No positive vesicles for TC21 and CD3ζ coming from the IS were detected (n=4 for each mutant). However, both TC21 mutants co-localized with CD3ζ at the IS. Scale bars-5 μm. The colocalization of TC21 S28N with CD3ζ at the IS was constant and similar at early time points after the first contact and at late time points, with average PC of +0.790±0.021 and average ICQ of +0.320±0.019 (n=4). The colocalization of

CD3ζ TC21 G23V at the IS was lower than for the S28N mutant, with average PC of +0.548±0.030 and average ICQ of +0.208±0.020 at late time points (~20 min). **(D)** Intensity correlation analysis of CD3ζ and RhoG. Jurkat cells were co-transfected with CD3ζ-Cherry and RhoG-GFP and stimulated with SEE-loaded Raji cells. Conjugated formation was recorded by confocal microscopy taking different time points and co-localization analysis were performed as in panel A. Both proteins seem to co-localize at the IS 5-10 min after the initial contact and begin to be co-internalized from the IS after that. Average values obtained at the IS for times longer than 5 min after ICA were PC of +0.676±0.026 and ICQ of +0.236±0.015 for n=8. For ICA values in internalized vesicles we took large areas of the cytoplasm beneath the IS, such as it is shown for area 1 at time 25.5 min. Scale bar-5 μm. These areas were selected on the basis of being originated in the IS, as evidenced in the time-lapse videos (movies not shown). In these areas there were vesicles showing co-localization of both markers and zones in which such co-localization was not evident. Nevertheless, the average values (PC= +0.144±0.033; ICQ= 0.025±0.009) for n=6 indicated a significant co-localization.

Suppl. Fig. S2. The TC21-dependent internalization of the TCR from the IS is clathrin-independent. **(A, B)** Intensity correlation analysis. Jurkat cells were co-transfected with TC21-GFP and CD3ζ-Cherry and stimulated with SEE-loaded Raji cells for 30 min. Alexa633-labeled transferrin (blue) was added during the last 5 minutes (A). Alternatively, cells were stained in blue after fixation and permeabilization with an anti-clathrin heavy chain (CHC) antibody (B). Scatter plots and (A-a)(B-b) plots are shown for the whole area placed immediately below the IS (area 1) and for individual vesicles (vesicle 2) double positive for TC21 and CD3ζ. PC and ICQ data were generated for TC21 and CD3ζ double positive vesicles and compared with transferrin (A, n=8) and

CHC (B, n=12) values. Black bars represent the PC and ICQ values for TC21 and CD3ζ co-localization, white bars for CD3ζ and either transferrin or CHC co-localization, and grey bars for TC21 and either transferrin or CHC co-localization. **(C)** Knockdown of clathrin heavy chain. Jurkat cells were transfected with a mixture of two siRNAs for CHC (see Supplemental Experimental Procedures) or mock transfected (control) and the effect on deprivation of CHC protein was analyzed by immunoblotting with the anti-CHC antibody. The membrane was reprobed with anti-GAPDH (glyceraldehide phosphate dehydrogenase) as loading control. Quantification of the intensity of the bands was carried out as for Fig. 7B. **(D)** Transferrin endocytosis assay. Non-transfected Jurkat control cells were incubated for 5 min on ice with Alexa633-labeled transferrin and then subjected or not to an acidic 2 min wash with 150 mM glycine pH= 3.0 (left). Endocytosis is prevented at 0ºC and the acidic treatment resulted in the removal of most of the bound transferrin. Another experiment was performed in parallel in which mock transfected control or siRNA-transfected (KD) Jurkat cells were incubated with Alexa633-labeled transferrin for 5 min at 37ºC and then subjected to acidic wash (right). The control cells had completely endocytosed transferrin since their fluorescence did not diminish upon acidic treatment. However, in CHC knockdown cells fluorescence intensity was diminished to values close to those of cells incubated on ice, indicating that transferrin was not endocytosed. **(E)** TCR downregulation was partly inhibited in CHC knockdown cells. Jurkat cells were mock-transfected (control) or transfected with the siRNA mixture for CHC (CHC KD) and stimulated for different time points with SEE-loaded Raji APCs. The remaining TCR surface expression was evaluated by flow cytometry. **(F,G)** TC21-dependent TCR internalization from the IS is clathrin-independent. Jurkat cells were mock-transfected or transfected with the CHC siRNA mixture and 48 h later transfected with TC21-GFP and CD3ζ-Cherry and stimulated

with SEE-loaded Raji cells. Panel F illustrates how TC21 and CD3ζ are co-internalized in a CHC-depleted cell 9.5 min after stimulation; the intensity correlation analysis is shown to the right. Panel G shows the quantification of clathrin depletion effect on TCR/TC21 co-internalization from the IS. After fixation, the number of Jurkat:Raji cell conjugates with double positive ($TC21^+$ $CD3\zeta^+$) internal vesicles just below the IS was counted in triplicate samples of n=16 cells. Data shown as mean±SEM.

Suppl. Figure S3. **(A)** Endocytosed TCR and TC21 co-localize with endosomal and phagosomal markers. Jurkat cells co-transfected with TC21-CFP, CD3ζ-Cherry and either of the GFP-tagged Rab GTPases (Rab4, Rab5, Rab7 and Rab11) were stimulated with SEE-loaded Raji for 5 (Rab4, Rab5) or 15 (Rab7, Rab11) min. The colors of the markers were shifted for convenience. The presence of internal vesicles positive for the three markers is indicated with arrowheads. Representative of 20 cells visualized in 3 experiments. **(B)** T cells phagocytose anti-CD3-coated beads in a TCR-dependent manner. Jurkat T cells and the TCR negative Jurkat mutant clone 31-13 were incubated for 60 min with 1 μm latex beads coated with either the anti-CD3 OKT3 antibody or with the isotype-matched anti-CD8 OKT8. After fixation, the cells were permeabilized and stained with a secondary anti-mouse Ig-Alexa 594 antibody (red) to visualize the beads, and with FITC-labeled phalloidin to visualize the contour of the cell. Since Jurkat cells are CD8 negative, incubation with the OKT8-coated beads serves as a negative control. Representative of 4 experiments. **(C)** Engagement of the TCR but not of another membrane receptor (transferrin receptor) triggers phagocytosis. Wild type Jurkat cells were incubated for 60 min with 1 μm red fluorescent beads coated with either anti-CD3 (OKT3) or with the anti-transferrin receptor (TfR, FG1/16). To distinguish phagocytosed from adhered beads, cells were incubated before

permeabilization with a green (Alexa 488)-fluorescent anti-Ig antibody. After permeabilization, cells were also stained with FITC-labeled phalloidin. The cell cortex appears green due to the presence of polymerized F-actin, while adhered beads appear yellow because they were accessible to the anti-Ig antibody and phagocytosed beads are red. Representative of 3 experiments. **(D)** Flow cytometry quantification of the aforementioned experiments. Wild type (Jk) or the TCR negative Jurkat mutant 31-13 cells were incubated with 1 μm latex beads coated with the indicated anti-CD3, anti-CD8 or anti-TfR antibodies for the times indicated at a 40:1 ratio (bead:cell) at 37ºC. Non-internalized beads were removed after a two-minute acidic wash and cells were then fixed and permeabilized before staining with a secondary Alexa 488 anti-mouse Ig antibody. Bead phagocytosis was quantified by flow cytometry. Representative of 3 experiments.

Suppl. Figure S4. Effect of TC21 and RhoG deficiency on antigen- and anti-CD3 bead-triggered T cell activation. **(A, B & C)** $CD4^+$ T cells genetically deficient in TC21 or RhoG show enhanced CD69 expression and IL-2 secretion in response to antigen, coupled with reduced T cell proliferation. AND T cells of the indicated genotypes were stimulated with the concentrations of MCC antigen indicated for 24 h (for CD69 and IL-2) or 72 h to assess proliferation. Each value represents the mean and standard deviation of three datasets. *$P < 0.05$, and **$P < 0.005$ (two-tailed Mann-Whitney test). Representative of 3 experiments. **(D & E)** Increased intensity of proximal TCR signals in TC21- and RhoG-deficient $CD4^+$ T cells. AND T cells of the indicated genotypes were incubated for the times indicated with DCEK APCs preloaded with 10 μM MCC. Total cell lysates were resolved by SDS-PAGE and examined in western blots (WB) probed with the antibodies indicated. The molecular weight of markers run in parallel

are indicated on the right. Representative of 3 experiments. **(F & G)** T cells of the indicated genotypes were stimulated with the indicated number of anti-CD3-coated latex beads of the indicated sizes for 24 h to assess CD69 expression (panel F) or 72 h (panel G) to assess proliferation. Each value represents the mean and standard deviation of three datasets. *$P < 0.05$, and **$P < 0.005$ (two-tailed Mann-Whitney test).

Suppl. Figure S5. TC21 and RhoG mediate TCR downregulation provoked by immobilized anti-CD3 but not by soluble antibody. **(A)** TCR downregulation after stimulation for 12 h with the indicated concentrations of either plastic-bound or soluble anti-CD3 antibody 145-2C11. Each value represents the mean and standard deviation of three datasets. *$P < 0.05$, and ***$P < 0.0005$ (two-tailed Mann-Whitney test); n.s., not significant. **(B)** T cell proliferation after stimulation for 72 h with the indicated concentrations of either plastic-bound or soluble anti-CD3 antibody 145-2C11. Each value represents the mean and standard deviation of three datasets. ***$P < 0.0005$ (two-tailed Mann-Whitney test); n.s., not significant.

Suppl. Figure S6. The immunological synapse is reminiscent of a frustrated phagocytotic process. **(A)** Phagocytosis of a large particle coated with a TCR ligand (diamonds). The TCR is triggered in a zipper-like manner, promoting a wave of actin polymerization (green band) that extends the plasma membrane around the particle. This results in the tight apposition of the T cell membrane to the particle, which is eventually phagocytosed. **(B)** When the APC is too large to be phagocytosed, the T cell extends its membrane on the APC in a movement triggered by the TCRs as they are engaged by pMHC (diamonds), resulting in an actin wave (green). The actin wave tends to be wider and wider until maximal T cell:APC membrane apposition is reached (1). The engaged TCRs signal in peripheral microclusters (represented as dimers here)

which tend to coalesce at the center of the structure (cSMAC). The centripetal transport of the TCR promotes a retraction of the actin ring (2) that serves to close the T cell's plasma membrane around a protrusion of the APC membrane, which is extruded by the T cell. The frustrated phagocytosis of the whole APC by the T cell leads to the phagocytosis (trogocytosis) of a patch of the APC membrane and the internalization of the TCR from the IS (3).

Suppl. movie 1. Time-lapse videomicroscopy of Jurkat cells transfected with CD3ζ-YFP and TC21-CFP, and stimulated with superantigen SEE-loaded Raji APCs. Raji cells expressed the red fluorescent protein DsRed and are pseudocolored in blue. Two sequentially contacting Raji APCs appear in the video. TC21-CFP emission is shown in red and that of CD3ζ-YFP is in green.

Suppl. movie 2. Time-lapse videomicroscopy of Jurkat cells transfected with CD3ζ-DsRed (in red) and wild type RhoG fused to GFP (in green) and stimulated with superantigen SEE-loaded Raji APCs. The top two panels of the movie have been pseudocolored to indicate the intensity of TCR accumulation (top left) and RhoG accumulation (top right). The color scale goes from low intensity (purple-blue) to high (red) and highest (white) intensities.

Suppl. movie 3. Time-lapse videomicroscopy of Jurkat cells transfected with TC21-DsRed and the dominant negative mutant T17N of RhoG fused to GFP and stimulated with superantigen SEE-loaded Raji APCs.

Suppl. movie 4. Time-lapse videomicroscopy of wild type AND lymph node T cells transduced with a lentiviral vector expressing CD3ζ fused to GFP (green) and stimulated with MCC antigen-loaded DCEK APCs.

Suppl. movie 5. Time-lapse videomicroscopy of TC21-deficient AND lymph node T cells transduced with a lentiviral vector expressing CD3ζ fused to GFP (green) and stimulated with MCC antigen-loaded DCEK APCs.

Suppl. movie 6. Time-lapse videomicroscopy of RhoG-deficient AND lymph node T cells transduced with a lentiviral vector expressing CD3ζ fused to GFP (green) and stimulated with MCC antigen-loaded DCEK APCs.

Suppl. movie 7. Time-lapse videomicroscopy of wild type OT-I lymph node T cells transduced with a lentiviral vector expressing CD3ζ fused to GFP (green) and stimulated with OVAp antigen-loaded T2Kb APCs labeled red with PKH26.

Suppl. movie 8. Time-lapse videomicroscopy (overlap of the bright field and green channel images) of wild type non-transduced AND lymph node T cells stimulated with MCC antigen-loaded DCEK APC previously transfected with I-$E^K\alpha$-GFP.